AD_____

Award Number: W81XWH-10-1-0609

TITLE: Neuroimaging of Brain Injuries and Disorders at Cleveland Clinic

PRINCIPAL INVESTIGATOR: Stephen M. Rao, Ph.D.

CONTRACTING ORGANIZATION: Cleveland Clinic Foundation
Cleveland OH 44195

REPORT DATE: December 2013

TYPE OF REPORT: Final

PREPARED FOR: U.S. Army Medical Research and Materiel Command
Fort Detrick, Maryland 21702-5012

DISTRIBUTION STATEMENT:

Approved for public release; distribution unlimited

REPORT DOCUMENTATION PAGE

Form Approved
OMB No. 0704-0188

1. REPORT DATE *(DD-MM-YYYY)*	**2. REPORT TYPE**	**3. DATES COVERED** *(From - To)*
December 2013	Final	23 September 2010 - 22 September 2013

4. TITLE AND SUBTITLE

Neuroimaging of Brain Injuries and Disorders at Cleveland Clinic

5a. CONTRACT NUMBER

5b. GRANT NUMBER
W81XWH-10-1-0609

5c. PROGRAM ELEMENT NUMBER

6. AUTHOR(S)

Stephen M. Rao, Ph.D.

Email: raos2@ccf.org

5d. PROJECT NUMBER

5e. TASK NUMBER

5f. WORK UNIT NUMBER

7. PERFORMING ORGANIZATION NAME(S) AND ADDRESS(ES)

Cleveland Clinic Foundation
9500 Euclid Avenue
Cleveland OH 44195

8. PERFORMING ORGANIZATION REPORT NUMBER

9. SPONSORING / MONITORING AGENCY NAME(S) AND ADDRESS(ES)

US Army Med Research Acq Act
820 Chandler Street
Fort Detrick, MD 21702-5014

10. SPONSOR/MONITOR'S ACRONYM(S)

11. SPONSOR/MONITOR'S REPORT NUMBER(S)

12. DISTRIBUTION / AVAILABILITY STATEMENT

Approved for public release; distribution unlimited

13. SUPPLEMENTARY NOTES

14. ABSTRACT

Blast injuries are the leading cause of injury in the Afghanistan and Iraq wars. It is unknown whether the neural and cognitive sequelae of blast-related traumatic brain injury (TBI) differs from those resulting from mechanically-induced TBI commonly observed in civilian accidents. Understanding the potentially unique sequelae of blast-related TBI is critical for accurate diagnosis and designing effective pharmacological and neurorehabilitation interventions. Functional MRI is an imaging method that detects increases in cerebral blood volume, flow, and oxygenation that occur locally in response to increased neuronal activity. Recent work has shown that fMRI is capable of measuring synchronous spontaneous low-frequency BOLD fluctuations (LFBFs) in the human brain during a state of alert rest. These spontaneous fluctuations are correlated in brain regions with a high degree of connectivity. The LFBF measure of functional connectivity within the brain is proving to be a powerful and sensitive measure of pathology in a number of patient populations that have previously been difficult to study with other imaging methods. We have recently demonstrated that LFBF measured functional connectivity can be combined with a structural measure of connectivity, MRI based diffusion tensor imaging/tractography, to enhance understanding of neuropathology in a patient population (Multiple Sclerosis).

15. SUBJECT TERMS

Blast-related traumatic brain injury (TBI), fMRI, DTI, cognition

16. SECURITY CLASSIFICATION OF:			**17. LIMITATION OF ABSTRACT**	**18. NUMBER OF PAGES**	**19a. NAME OF RESPONSIBLE PERSON**
a. REPORT	**b. ABSTRACT**	**c. THIS PAGE**			**19b. TELEPHONE NUMBER** *(include area code)*
U	U	U		12	

Standard Form 298 (Rev. 8-98)
Prescribed by ANSI Std. Z39.18

Table of Contents

INTRODUCTION

Blast injuries are the leading cause of injury in the Afghanistan and Iraq wars. In a study with Marine and Navy personnel wounded in action in Iraq during a one-month period in 2003, approximately 50% of the injuries were due to explosive devices. In an army medical facility, explosive devices and mortar were responsible for 88% of the wounded. Primary blast injuries occur when changes in atmospheric pressure cause organs containing air, such as the lung, bowel, and inner ear, to rupture. While the effects of primary blast on the brain have been considered to be the result of ruptured air emboli in blood vessels, primary blast may cause damage to the brain via other mechanisms. For example, blast to the abdomen may transfer kinetic energy from blast overpressure to the central nervous system via major blood vessels. Secondary blast injuries are caused by objects set into motion by the explosion, i.e., missiles, hitting people. Tertiary blast injuries are due to the whole body being set into motion by changes in air pressure and hitting objects. Quaternary, or miscellaneous, blast related injuries include crush injuries due to collapsed objects, burns, and smoke inhalation. TBI can result from any of these categories of blast injury. While physiological and other effects of secondary and tertiary blast injury may be similar to those in mechanical TBI due to falls or motor vehicle accidents, effects contributed by primary blast to TBI are less known, although some similarities, such as edema and oxidative stress, common to mechanical TBI have been suggested in animal models. More than 50% of blast-related TBI fall within the mild to moderate severity range.

It is unknown whether the neural and cognitive sequelae of blast-related TBI differ from those resulting from mechanically-induced TBI commonly observed in civilian accidents. The pathophysiological mechanisms associated with TBI most commonly include bleeding, direct tissue damage, and diffuse axonal injury (DAI). The presence of a penetrating injury or intracerbral hemorrhage defines the severity of a TBI as at least moderate, but DAI can occur in the milder injuries. DAI results when sudden acceleration/deceleration and angular momentum forces cause shearing or stretching of axons, which can lead to impaired axonal transport. The microscopic result is the appearance of focal axonal swellings and subsequent axonal degeneration. DAI is common after closed head injuries and most commonly affects tracts at gray/white matter junctions, particularly in the frontal and temporal regions, but is often invisible on standard structural MRI. Understanding the potentially unique sequelae of blast-related TBI is critical for accurate diagnosis and designing effective pharmacological and neurorehabilitation interventions. A major goal of this project is to use advanced neuroimaging techniques and computerized neuropsychological assessment to determine if the long-term (> 12 month postinjury) brain sequelae associated with blast-related mild-to-moderate TBI (MTBI) can be distinguished from sequelae associated with civilian MTBI. To our knowledge, no such study has been reported in the literature.

BODY

The final year of the project was devoted to completion of image analyses and analyses of the neurobehavioral data. To summarize, T1-weighted anatomic MRI, motor fMRI, resting-state fMRI (rs-fMRI) and HARDI DTI were acquired in four groups of 15 subjects each: military TBI (milTBI), civilian TBI (civTBI), military controls (milCON), and civilian controls (civCON). The groups were matched on age and education:

		Age		Education	
	n	mean	sd	mean	sd
civCON	15	29.1	4.8	13.8	2.3
civTBI	15	27.1	5.1	14.9	1.5
milCON	15	27.1	2.5	14.1	2.4
milTBI	15	28.7	6.3	13.3	1.8

We established minimum performance criteria and minimum motion limits for fMRI, rs-fMRI and DTI as described in Lowe et al. (2008) for the hand motor task. In general, these were very well-performing subjects, both on the task and with minimal head motion, in all groups. Only three subjects (out of 64 total acquired) were discarded for excessive motion during the rs-fMRI scan sessions, and none were discarded for poor behavioral performance on the finger tapping fMRI scan. One subject was excluded due to significantly different anatomy from the group (large ventricles). This resulted in a total of 60 subjects listed in the table above.

This report covers the functional and structural connectivity aims of the grant, and the analyses undertaken to address these aims. Ultimately no significant effects were observed, and several additional analyses were performed to verify this finding. Several novel methods were developed and one new method is being investigated on an ongoing basis for functional connectivity in the data acquired under this study. We report here on the data analyses performed to satisfy our aims, the findings obtained and new methods developed in the course of analysis.

Hypothesis 1: *On LFBF scanning, functional connectivity between frontal lobe premotor regions will be reduced in chronic TBI relative to control participants*. For the LFBF analysis, a 2 (Military vs. Civilian) x 2 (TBI vs. CON) factorial ANOVA will be performed on the Fc measure to examine main and interaction effects.

Hypothesis 1 methods and analyses:

For the functional connectivity measurements of Aim 1, we had proposed seed-based functional connectivity as described in the Project Narrative and Lowe et al 2008. Briefly, for each subject, we performed the following steps.

1. The hand motor region was identified on the T1 anatomic and a region of interest (ROI) drawn on the gyrus corresponding to the hand motor area and premotor cortex on each side of the brain.
2. These ROIs were transformed to the hand motor task fMRI scan data.
3. The statistical activation fMRI map was used to identify the most task-active single-voxel brain locations in each ROI.
4. These single-voxel locations were transferred to separate scans acquired in that subject for rs-fMRI and DTI, using an appropriate spatial coregistration.
5. rs-fMRI data was corrected as described in the Project Narrative. Subsequently,
    a. The coregistered identified voxel location was expanded to a nine-voxel ROI centered on the most activated location in rs-fMRI data.
    b. A cerebrospinal fluid mask (described below) was used to exclude regions of non-brain tissue, while checking the total number of seed voxels.
    c. The average timeseries at each brain region was computed and temporally low-pass filtered to < 0.08Hz (Lowe et al 1998).
    d. The coherence of low frequency BOLD fluctuations between homologous brain regions was computed by taking the Pearson linear correlation coefficient.
    e. The cross-correlation is converted to a Student's t (Lowe et al 1999).

f. The number of voxels above a P<0.05 significance threshold in the z-score connectivity map is stored as F_c
g. The whole-brain correlation map for a pathway is z-score corrected by fitting a normal distribution to the full-width at half-maximum of the Student's t's for all voxels (Lowe et al 1998), and the resulting map is saved.

Group comparison: The z-scored F_c maps were passed to a 2 (civ vs mil) x 2 (OI vs TBI) voxelwise ANOVA and examined for significance. There were no findings that exceeded significance. Separately, on a subset of data, a 2-way ANOVA was performed (mil vs civ TBI) to examine if there were any subtle main effects that could be obscured by the more demanding significance requirements of a 2x2 ANOVA. Figure 1 shows a) the mean of all military TBI (blast-TBI) subjects, b) the mean of all civilian TBI (non blast-TBI) and c) ANOVA of blast- vs non blast-TBI. Subcortical connectivity (bilateral thalamus, left caudate) to the motor cortex was observed to be increased in the blast-TBI group. These findings, however, were not significant after correction for multiple comparisons.

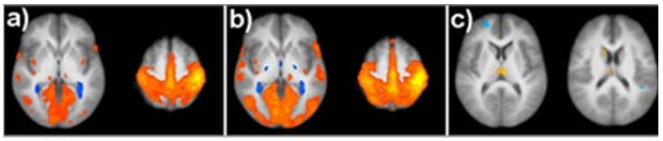

Figure 1

Cerebrospinal fluid (CSF) mask method: The echoplanar pulse sequence used to obtain the rs-fMRI and fMRI scans was modified to acquire the unsaturated volumes at the start of the scan. These scans are typically not acquired while the first few volumes are excited, as the signal level changes dramatically as the water tissue signal evolves to a steady state equilibrium. We discard these images from our analysis as well, but the first four volumes in particular can be used to make a distortion-matched CSF mask. CSF has a much greater signal change across the first few volumes than other tissue types, and simply applying an appropriate threshold to a ratiometric image (first image to average of images 2-4), we can identify CSF robustly with the same distortion as the rs-fMRI scan. This is an improvement over anatomic mask methods because an anatomically-derived mask does not share the same warping and furthermore must be coregistered to the EPI scans, resulting in substantial error in pixel CSF identification.

Figure 2 shows CSF mask creation and overlay on EPI

Additional functional connectivity analyses: Given the differences expected, and the relative quality of this dataset, we were concerned that the methods used could be a possible reason for the lack of group differences, so we explored several variations on the functional connectivity methods.

Alternative F_c method 1: The most task-activated voxels on both sides may not be the most connected voxels. It is possible that interhemispheric motor connectivity may be greatest between the most task-activated primary motor cortex voxel on one side to a slightly adjacent region on the opposite primary motor cortex. A large part of the interhemispheric communication is expected to be inhibitory in nature and may synapse at a separate cortical area nearby for further processing before reaching the most activated location. Thus, we implemented a search for the maximum connectivity within the contralateral motor ROI. For this method, it is likely important to restrict the search area carefully, so all motor ROIs underwent a second round of editing to ensure no tissue outside the motor area was covered. Then we performed a simple search over maximum connectivity between one side max-activated 9-voxel seed and each contralateral 9-voxel seed centered on each voxel in the ROI. This method did not result in significant group differences.

Alternative F_c method 2: Based on similar reasoning, it is possible that the most functionally connected voxels in the motor system are those with the strongest interhemispheric pathway track

density. For this reason, we explored further adjustment of the fc ROIs based on the probabilistic track density for the motor pathway. In this case, a voxel in the midline corpus callosum within the previously-defined motor pathway was used as a start point, with contralateral motor ROIs as endpoints. To identify the endpoints, the maximum track density that was within the motor ROI and closest to the voxel of highest track density was saved as the most structurally connected voxels. Then a 9-voxel seed was placed on both sides centered over these most structurally connected voxels. This method did not result in significant group differences.

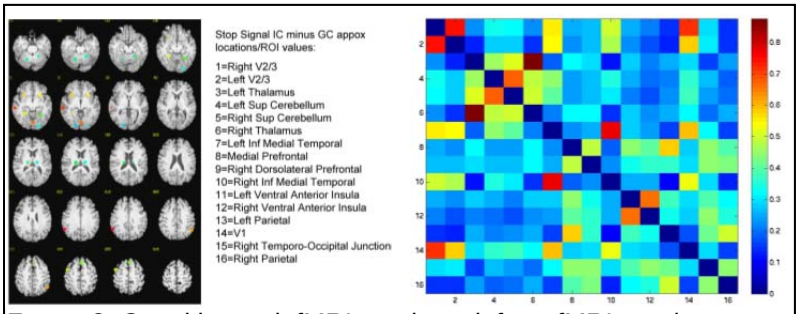

Figure 3: Cognitive task fMRI seeds on left, rs-fMRI matrix between these seeds on right, showing full network connectivity

Alternative F_c method 3: With our failure to find a result in motor connectivity, we concluded that a likely reason was our pathway was too specific. Fortunately, we had been acquiring an additional fMRI scan using a stop-signal task in these subjects, which would allow us to probe cognitive regions. The stop-signal task requires subjects to press a button when instructed by visual stimulus (Go trials). For some of the trials a second instruction was given that indicated the subject should inhibit pressing the button (Inhibit trials). The behavioral performance from button presses enabled the separation of events into Go-Correct, Go-Incorrect, Inhibit-Correct and Inhibit-Incorrect events. Minimum performance criteria was used to remove subject data with too many or too few of the appropriate events. From the group-averaged stop-signal Inhibit-Correct minus Go-Correct fMRI activation, and appropriate thresholding, we obtained brain regions related to task inhibition (Figure 3). These were segmented into clusters and converted into spherical ROIs on 16 brain regions. The rs-fMRI matrix was compared across TBI and OI groups, and with blast vs no blast TBI. No test achieved significance after correcting for multiple comparisons..

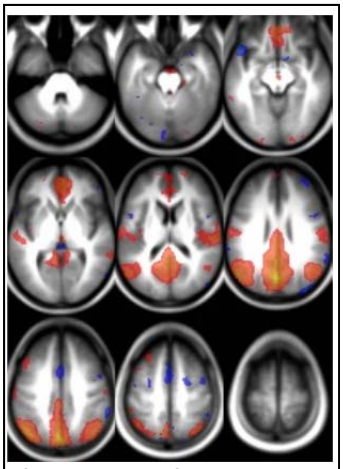
Figure 4: Resting state network from ICA decomposition of all subjects' rs-fMRI data in MNI standard brain space.

Alternative F_c method 4: We turned to a data-driven analysis method to allow us to investigate an entire network comprising several areas throughout the brain. In particular, we compared the "default mode network" (DMN), so named for the tendency of key regions included in this network to down-regulate blood flow during the performance of various tasks (Figure 4). The DMN has been shown to be affected by TBI and includes distributed regions connected by long-range white matter pathways. It was expected that we may have a larger effect size from TBI with this network. The network map derived from the group concatenated data was back-projected to individual subject data to derive subject-specific DMNs, which are noisier and less robust than that derived from a large group concatenated dataset but which are then relevant for individual subjects. The relative strength of each subject's DMN in the posterior cingulate was computed and this was compared across groups. No significant group differences emerged.

Hypothesis 2: *DTI changes, characterized by lower FA and higher MD at the gray-white junction, corpus callosum, central semiovale, and internal capsule will be seen in TBI but not in Control subjects.*

DTI data were first processed using the Tract-Based Spatial Statistics (TBSS) program within the FSL 4.0 image processing software package (http://www.fmrib.ox.ac.uk/fsl/tbss/index.html) to create a mean white matter skeleton. Specifically, all FA images were aligned to a cubic 1 mm standard space and the FMRIB58 standard image. FA images were averaged and a skeleton created with an

FA threshold of 0.2 representing tracts common to all participants. This method of "thinning" each white matter tract perpendicular to the tract and thresholding FA helps to eliminate partial volume effects and areas of high inter-subject variability. Each participant's maximum FA value from the nearest relevant tract center was assigned to the corresponding skeleton voxel, which corrects for residual misalignments after nonlinear registration.

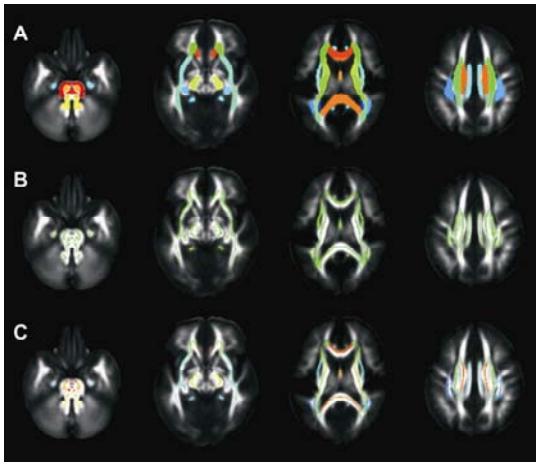

Figure 5. Illustration of method for merging TBSS-derived skeleton with ICBM-DTI-81 white matter tract atlas

Following the creation of the FA skeleton, white matter tracts of interest were created using the ICBM DTI-81 white matter atlas. This atlas is based on probabilistic tensor maps derived from 81 healthy subjects and consists of 48 white matter tracts with high intra- and inter-rater reliability. Using the Analysis of Functional NeuroImages (AFNI) software package, the TBSS-derived FA skeleton was overlaid onto the ICBM DTI-81 atlas (see Figure 5). From this conjunction map, mean FA, MD, DA, and DR values were calculated for each subject for each white matter tract of interest. Two-way ANOVAs (TBI/CON vs civ/mil) were performed to assess group differences for each white matter tract and each DTI parameter (FA, MD, DA, and DR). The false discovery rate (FDR) method was performed separately for each DTI parameter to control for multiple comparisons. Post hoc analyses were conducted using Tukey HSD.

No significant main (TBI vs. CON, mil vs. con) or interaction effects survived the FDR correction for any of the 48 white matter tracts and DTI parameters.

Hypothesis 3: *Decreased LFBF connectivity in chronic MTBI will be correlated with the location and severity of disrupted fiber tracks as measured by DTI.* In the civCON subjects, tractography will be used to identify connections between motor and premotor ROI's identified in fMRI activation scans. These connection models will be then be applied to the TBI patients to determine if lower functional connectivity is associated with greater disruption of white matter tracts. Multiple regression analysis will be used to test these associations, with severity of PTSD symptoms considered as a covariate.

<u>Hypothesis 3 methods and analyses:</u>

For the functional and structural connectivity measurements of Aim 3, we followed the seed-based functional connectivity method described above and structural connectivity measurements as described in the Project Narrative. Essentially the same fMRI activation location information used for rs-fMRI was used to localize DTI tract start and end points.

1. DTI data was corrected as described in the Project Narrative.
2. An additional novel method using inverted phase-encode spin echo acquisitions to obtain the exact static field spatial warping was used to unwarp the DTI images such that they would match anatomic images. The most-activated voxel locations were unchanged by the unwarping due to minimal static warping in the motor cortices.
3. A white matter mask created from the T1-weighted anatomic image was coregistered to DTI data.
4. This optimized static unwarping was incorporated into our existing iterative affine combined eddy current and motion correction pipeline (Sakaie et al 2007). Subsequently,

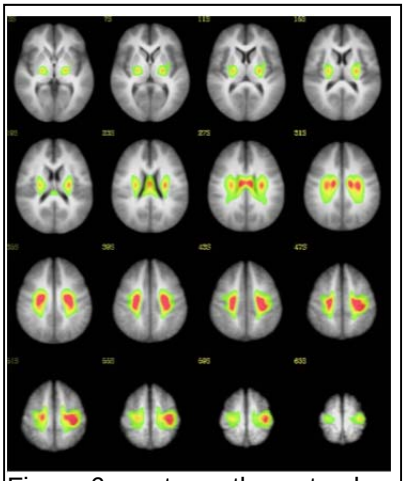
Figure 6: motor pathway track density images, overlain on anatomy. Note paths through corpus callosum and down through thalamus.

a. The 71 directions of diffusion images, two averages, were fitted to a tensor fiber orientation distribution (FOD) model and several metrics computed: fractional anisotropy (FA), transverse diffusivity (TD), mean diffusivity (MD) and longitudinal diffusivity (LD).
b. The most task-active location in homologous brain regions in DTI data were used as starting and end points for probabilistic tractography, using 1 million tracks. Tractography incorporated the voxelwise fitted FOD with a manually edited and verified midline mask and white matter mask. This results in a pathway track density map. This was done for each pathway, so left primary motor to right primary motor is the motor pathway (Figure 6).
c. For each pathway, the diffusivity parameters were integrated over the number of tracks in each voxel, giving an accurate and robust measure of FA, TD, MD and LD.

Initial Analysis comparing F_c with structural connectivity: We first attempted to reproduce the linkage between F_c and structural connectivity as observed previously (Lowe et al 2008). Methods were as described above and in Lowe et al 2008. See Figure 7, which shows an extension of our previous finding in MS patients and the reproduced analysis in this data. Note the large difference in effect size, indicating a surprising lack of range in diffusivity parameters in TBI subjects and controls.

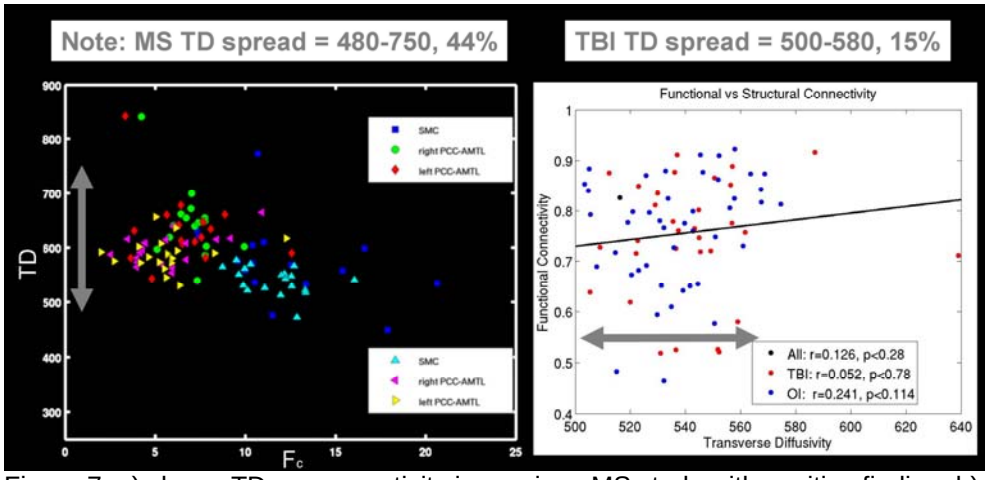

Figure 7: a) shows TD vs connectivity in previous MS study with positive finding, b) shows connectivity vs TD in present study. Note the difference in effect size, low spread in TD in TBI.

<u>Group comparison:</u> Because of difficulty with findings in LFBF analyses, the DTI data was analyzed separately globally for differences between groups. No significant group differences emerged.

<u>Static unwarping method:</u> Recently, a method was developed to unwarp spin-echo EPI images (used for DTI) such that the final images have no apparent warping in them and result in a visually perfect match to anatomic MRI images. This method requires the acquisition of a second, nearly identical image, with the only difference being an inversion of the phase-encoding axis for this second image. Inversion of the phase-encoding axis results in an inversion of the direction of image warping, so the true location of MR signal is exactly between two shifted signals. We modified a spin-echo EPI sequence to acquire matched inverted phase-encode images immediately prior to DTI for each subject and subsequently used this method to produce a static unwarping map for DTI (Figure 8). Because we expect some head motion during DTI, we have long used a combined eddy current and motion correction method to improve data quality. However, the orientation of the shift changes with head position, so the shiftmap should be adjusted to the inverse of the first-pass motion correction parameters. In this way, the shiftmap has a simulated motion, and each raw DTI image can be unwarped. There is a second

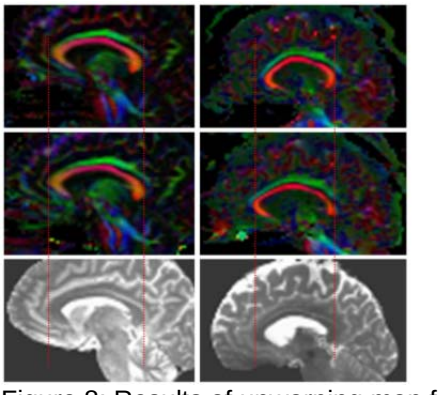

Figure 8: Results of unwarping map for DTI.

order effect in that the field homogeneity itself changes with head position, but this is a much smaller effect that is outside the scope of this effort. The result of the unwarping is an improvement in tensor fit – the fit error is reduced on average by 15%, resulting in improved pathway specificity. This method did not result in improved detection of group differences.

Hypothesis 4: *Performance on computerized neuropsychological testing (ANAM) will better discriminate TBI from Control participants than standard paper-and pencil tests.*

The table below summarizes the analyses of the standard paper-and pencil tests:

					2 x 2 ANOVA		
Variable	**milTBI**	**milCON**	**civTBI**	**civCON**	**TBI vs CON**	**Mil vs Civ**	**Interaction**
Neuropsychological Testing							
Trails A - sec	26.5 (10.5)*	23.9 (4.6)	22.0 (7.2)	23.0 (9.7)	-	-	-
Trails B - sec	65.5 (41.1)	60.6 (26.8)	50.6 (20.0)	59.0 (28.9)	-	-	-
Trails B-A - sec	39.0 (34.2)	36.6 (24.5)	28.5 (19.1)	35.9 (25.4)	-	-	-
COWAT - total	36.9 (9.5)	36.9 (9.0)	43.6 (9.8)	43.6 (15.0)	-	0.007** (Mil < Civ)	-
CVLT Short Delay - total	9.6 (3.4)	10.2 (3.1)	11.6 (1.7)	10.7 (2.2)	-	0.030 (Mil < Civ)	-
CVLT Long Delay - total	9.4 (3.9)	10.8 (3.1)	12.0 (1.7)	10.6 (2.3)	-	-	0.041***
CVLT - T-score	50.4 (7.9)	49.6 (8.9)	52.2 (7.7)	52.5 (6.4)	-	-	-
SDMT - total written correct	51.5 (12.5)	58.2 (8.7)	61.8 (15.1)	61.2 (9.6)	-	0.010 (Mil < Civ)	-
SDMT - total oral correct	61.2 (13.7)	66.0 (11.1)	68.8 (16.3)	71.9 (12.1)	-	0.024 (Mil < Civ)	-

As predicted, these measures were not sensitive to detecting TBI effects. Several variables identified poorer performance in the military than civilian groups. One delayed verbal episodic memory measure (CVLT-long delay) identified an interaction between TBI/CON and civ/mil. This interaction, which did not survive a test of multiple comparisons, indicated that the blast milTBI group performed worse than the three other groups.

The next table summarizes the results of the computerized neuropsychological testing (ANAM):

					2 x 2 ANOVA		
Variable	**milTBI**	**milCON**	**civTBI**	**civCON**	**TBI vs CON**	**Mil vs Civ**	**Interaction**
ANAM Testing							
Stroop - Congruent							
Items Correct	29.8 (0.4)	29.9 (0.3)	29.9 (0.3)	30.0 (0.0)	-	-	-
Mean Reaction Time	801.9 (141.4)	733.4 (93.4)	755.5 (97.5)	771.1 (174.3)	-	-	-
SD Reaction Time	320.2 (308.2)	212.3 (52.0)	239.9 (153.6)	254.3 (227.7)	-	-	-
Stroop - Incongruent							
Items Correct	21.8 (11.7)	24.9 (10.3)	27.6 (7.4)	29.5 (0.8)	-	0.023 (mil < civ)	
Mean Reaction Time	967.3 (566.0)	894.7 (481.8)	921.8 (162.2)	1034.4 (313.2)	-	-	-
SD Reaction Time	371.2 (377.2)	295.3 (221.7)	282.3 (167.5)	407.7 (264.1)	-	-	-
Go-NoGo							
Items Correct	59.3 (1.1)	59.8 (0.4)	59.7 (0.6)	59.5 (1.0)	-	-	-
Items Incorrect	2.8 (2.5)	1.1 (1.1)	0.9 (1.1)	3.9 (6.4)	-	-	0.011
Mean Reaction Time	409.2 (54.6)	407.5 (48.2)	413.9 (56.3)	388.6 (45.6)	-	-	-
Code Sub							
Items Correct	68.7 (2.9)	71.3 (0.8)	70.7 (1.9)	70.9 (1.2)	0.007 (TBI < CON)	-	0.020
Mean Reaction Time	1316.9 (333.0)	1135.5 (249.6)	1193.5 (203.0)	1198.8 (336.0)	-	-	-
SD Reaction Time	487.6 (268.1)	369.0 (181.4)	403.0 (178.1)	399.5 (160.6)	-	-	-
Code Sub Recall							
Items Correct	16.6 (1.6)	17.5 (1.1)	17.5 (0.8)	17.4 (1.4)	-	-	-
Mean Reaction Time	1284.5 (270.9)	1170.8 (243.7)	1163.2 (314.8)	1250.3 (306.3)	-	-	-
SD Reaction Time	581.9 (387.9)	450.6 (324.7)	591.1 (515.3)	553.7 (283.1)	-	-	-
Running Memory							
Accuracy %	87.5 (14.0)	96.7 (3.2)	95.2 (4.3)	92.6 (10.1)	-	-	0.014
Mean Reaction Time	614.7 (103.7)	592.1 (82.0)	614.6 (83.3)	627.5 (104.4)	-	-	-
SD Reaction Time	142.6 (24.6)	111.9 (12.8)	122.3 (26.4)	136.5 (37.2)	-	-	0.002

On the ANAM, one variable distinguished TBI from controls: total items correct on the Code Substitution task. Four measures demonstrated significant interactions between TBI/CON and mil/civ: items incorrect on the Go-NoGo task, total items correct on the Code Substitution task, and percent accuracy and the reaction time standard deviation on the Running Memory task. In all cases, the blast milTBI group performed worse than the three other groups. It would appear that the ANAM was slightly more sensitive than standard paper-and pencil tests for detecting groups differences that suggest greater cognitive impairment in TBI subjects exposed to blast

Hypothesis 5: *The combination of LFBF, DTI, and ANAM will better discriminate blast TBI from mechanical TBI than each individual method.*

In light of the negative group findings associated with the LFBF and DTI analyses, we did not think it prudent to conduct these analyses.

KEY RESEARCH ACCOMPLISHMENTS

The key accomplishments can be summarized as follows:

- Hit our target enrollment of 60 subjects (15 per group).
- All MRI scans and neurobehavioral testing acquired without technical problems.
- ANAM testing revealed poorer performance on cognitive testing on milTBI subjects exposed to blast than civTBI subjects who experienced mechanical TBI.

REPORTABLE OUTCOMES

Presentations:

E. B. Beall, S. M Rao, M.D. Phillips, M. J. Lowe, Functional Connectivity differences in Blast-Induced vs. non-Blast- Induced Traumatic Brain Injury. Organization for Human Brain Mapping 12th Annual Meeting, Beijing, June 10-14, 2012.

E. B. Beall, S.M. Rao, M.D. Phillips, M. J. Lowe, Functional Connectivity in Blast-Induced vs. non-Blast-Induced Traumatic Brain Injury. 20th Annual Meeting of the International Society for Magnetic Resonance in Medicine. Melbourne, May 6-11, 2012.

Cleveland Clinic personnel receiving pay from research effort:

Stephen Rao
Mark Lowe
Ken Sakaie
Stephen Jones
Michael Parsons
Erik Beall
Michael Phillips
Jian Lin
Christine Reece
Alex Bura
Juliet Schulz
Svetlana Primak
Lyla Mourany
Michael Lengen

CONCLUSION

Despite multiple approaches to the analysis of LFBF and DTI measures, we were unable to detect meaningful differences between TBI and Control subjects. We believe there are several possible explanations: 1) our original power analysis was incorrect indicating that we could see group differences with as little as 15 subjects per group, 2) the concussive injuries were too chronic (milTB = 52.9 months and civTBI = 29.7 months post-injury), and 3) analyses of LFBF and DTI measures are simply not sensitive to TBI effects in our sample. The ANAM test data proved to be specifically sensitive to blast injuries.

REFERENCES

None

APPENDICES

None

SUPPORTING DATA

None